Journal of Hydroinformatics

Journal of Hydroinformatics Vol 24 No 2, 481 doi: 10.2166/hydro.2022.169

Effect of ship-lock-induced surges on navigation safety in a branched lower approach channel system

Zhiyong Wan[a,b], Yun Li[a,b,*], Xiaogang Wang[b], Jianfeng An[b], Long Cheng[c] and Yipeng Liao[b,d]

[a] School of Water Resources and Hydropower Engineering, Wuhan University, Wuhan 430072, China
[b] State Key Laboratory of Hydrology-Water Resources and Hydraulic Engineering, Nanjing Hydraulic Research Institute, Nanjing 210029, China
[c] Lower Changjiang River Bureau of Hydrology and Water Resources Survey, Changjiang Water Resources Commission, Nanjing 210011, China
[d] College of Water Conservancy and Hydropower Engineering, Hohai University, Nanjing 210098, China
*Corresponding author. E-mail: yli@nhri.cn

ABSTRACT

Ships docking and traveling in a branched lower approach channel system are at risk from surges caused by multi-lane locks during emptying operations. For this reason, water-level variations in the lower approach channel in response to discharge, interval running time, and outlet location of lock operations were studied using a 2-D hydrodynamic model validated by physical model tests, and the impact of water level variation on navigation safety under extreme operation scenarios of a quadruple-lane lock group was identified. Results indicated that discharge and interval running time of lock emptying had the greatest impact on the water level variation at the lock head. Water level variation at the lower lock head of the ship lift exhibited a trend of first decreasing and then increasing with the increment of the discharge from the lock chamber into the outer river. Specifically, the surge height at the lock head of the ship lift reached the minimum when approximately 40% of the discharge generated by dual-lane locks during emptying operations was released into the outer river. Overall, the simultaneous operation of quadruple-lane lock group and unit load rejection should be avoided in engineering applications.

Key words: approach channel system, emptying operations, lock approach, ship lift, surges, water level fluctuations

HIGHLIGHTS

- A 2-D hydrodynamic model was utilized to analyze the water-level fluctuations in a branched approach channel system.
- Water-level fluctuations in response to discharge, interval running time, and emptying outlet location of lock operations were revealed in details.
- Extreme multi-lane lock operating scenarios were determined considering the requirement of safe docking of ships at the lower lock head of the ship lift.

GRAPHICAL ABSTRACT

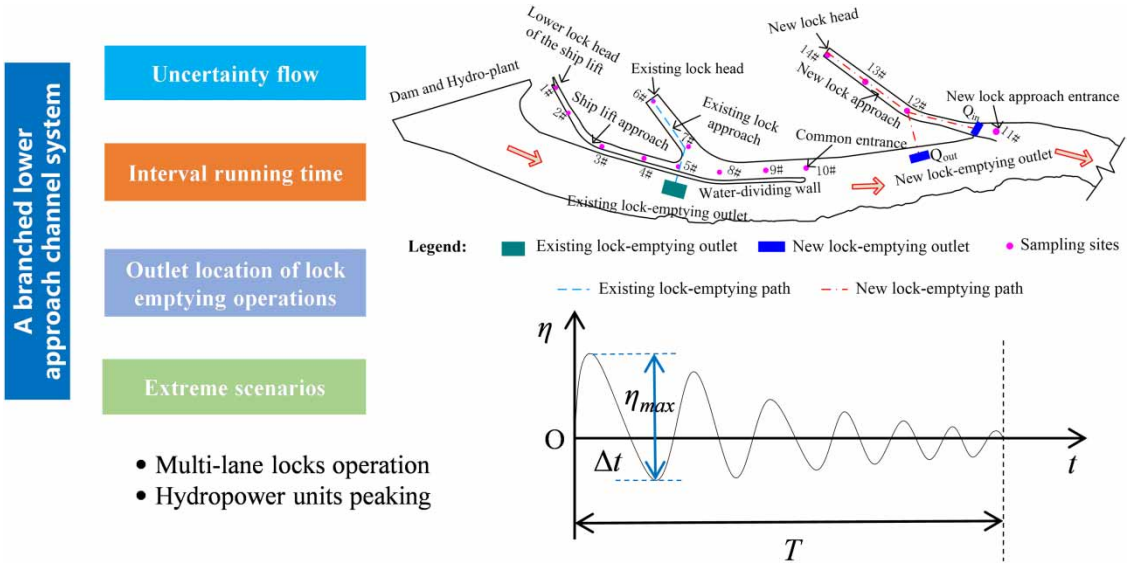

1. INTRODUCTION

Navigation locks are vital navigational architectures for overcoming water level differences upstream and downstream of rivers (Liang *et al.* 2014), as well as bridging upstream and downstream freight channels on inland waterways (McCartney 1986; PIANC 1995; MOTC 2001; MTPRC 2014; Wilschut *et al.* 2019). In recent years, with the growing demand for inland waterway shipping in China (Liao 2018; Deng *et al.* 2021), the number of single- and dual-lane locks has gradually increased, and the scale of a few ship locks has gradually begun to shift from single- and dual-lane to triple- and quadruple-lane. Nevertheless, with the increased number of lock accesses, to a certain extent, navigable flow conditions have turned into one of the major concerns for the shipping community in terms of the design and operation of any lock approach.

Unsteady flow resulting from an abrupt change in the flow rate from hydraulic structures (e.g., pumping station, spillway, ship lock, etc.) impacts the stabilization of water supply system (Baghlani 2014) and also alters navigable flow conditions (Liu *et al.* 2012; Zhang *et al.* 2019; Yang *et al.* 2020). The effects of dam discharge, hydropower unit regulations, lock operations, and other hub scheduling modes on the velocity, flow pattern, and surge in the channel are currently being investigated by domestic and international scholars using prototype observations, physical model tests, and numerical simulation techniques (Bravo & Jain 1991; Xue 1994; Stockstill *et al.* 2004; Maeck & Lorke 2014; Shang *et al.* 2017). Although prototype observations and physical model tests can enable visualization of navigable flow conditions, these are challenging and costly to implement effectively, especially for large scale models. However, in terms of hydrodynamic models, a one-dimensional model fails to reflect exactly the navigable flow conditions based on a handful of cross-sectional data; while a three-dimensional model occupies server memory resources and it has proven to be time-consuming. In modelling the waterway flow, a two-dimensional model based on the assumption of hydrostatic pressure is feasible and effective in actual engineering applications (Zhang *et al.* 2019). To sum up, a great deal of previous work has mainly focused on the navigable flow conditions in the shallow waterway. Nevertheless, when the surges evolve into an approach channel, the amplitude of water-level fluctuation is considerably greater than in the open waters, thereby posing a risk to ships passing through the navigation locks. On the one hand, insufficient water depth in the approach channel can readily result in the ship grounding; on the other side, a reverse water head may exhibit at the ship lock head due to a considerable surge height, endangering the structural safety of the mitre gates (Xu *et al.* 2018).

In the field of navigational hydraulics, the transient long-wave generated by a navigation lock filling and emptying system propagates in the approach channel or lock chamber (Natale & Savi 2000). To be specific, a negative surge is generated from the upstream approach channel when a navigation lock filling system equipped with culverts transfers water from an upper reservoir to the lock chamber (Schindfessel *et al.* 2014); conversely, when a lock emptying system equipped with culverts transfers water from the lock chamber to downstream river basin, a positive propulsion surge is observed in the approach channel (Zhou *et al.* 2005). In China, lock approach is a typically restricted channel characterized by narrow waters with a closed-end, small coefficient of cross-section, and low speed for vessel navigating. As a consequence, it is one of the

most complicated navigation channels in terms of navigable flow conditions. In particular, the evolution pattern of long-wave induced by ship lock during emptying operations has been studied via hydraulic model tests (Li & Sun 1999), and then relevant engineering initiatives to reduce surge height were proposed. However, the low navigation standard for a lock approach makes previous studies inapplicable to the current situation due to a small scale of the navigation lock and outdated lock operating systems in the past decades.

In recent years, freight traffic flow exhibits an upward trend in the inland navigation domain (Deng *et al.* 2021). With the increasing number of ship lock expansion projects, an increase in the number of lanes for ship locks may exacerbate water level fluctuations in the approach channel. However, on the one hand, most of the current studies on water-level fluctuations have merely focused on the single-lane lock or dual-lane lock approach rather than involving ship lift approach, and water level oscillations in the approach channel are insignificant under lock operations, thus lack of in-depth analysis of the lock operating conditions has gained little attention from the shipping community. On the other side, for a branched approach channel system, the surges generated by multi-lane locks operation evolve into the system accompanied by the transport of wave energy, and the complex boundary conditions cause the water level in the approach channel system to rise and fall periodically. Furthermore, investigation of water level fluctuations in a branched channel system induced by multi-lane locks during emptying operations has rarely been included in the current literature. In light of this, whether the changes in river flow under different combinations of lock operations have an impact on the safe navigation of the ship lift needs to be studied in depth. To be specific, due to the complexity of the relation between water-level fluctuations in the approach channel and the lock regulation mode, the surges in the approach channel during the emptying operation of the multi-lane locks should be examined systematically and thoroughly. Consequently, the objective of this study is to, using a branched lower approach channel system as a case study, investigate the relationship between the emptying operation modes of multi-lane navigation locks and maximum water level variation in the lower approach channel, in order to better understand the impact of the emptying operations of navigation lock on the navigable flow conditions in a branched lower approach channel system.

The remainder of this paper is structured as follows: Section 2 describes the layout of a typical branched lower approach channel system, the hydrodynamic model, and the definition of the maximum amplitude of water level fluctuations. Section 3 depicts the response of the water level variation to the discharge, interval running time, and outlet locations of ship lock during emptying operations. In addition, the extreme scenarios of a quadruple-lane lock group and hydropower unit operations are presented. Finally, the main conclusions drawn from this study are presented in Section 4.

2. MATERIALS AND METHODS

2.1. Layout of a typical branched lower approach channel system

A typical branched lower approach channel system on a long waterway is composed of a ship lift approach, an existing lock approach, and a new lock approach. The ship lift approach merges with the existing lock approach to constitute a common approach channel that connects to the main waterway. The bottom width of the lock approach is around 180–200 m, and the elevation of the riverbed is 56.5 m. The ship lift approach has a narrow cross-section and its width is around 80–90 m. In addition, a water-dividing dike with a stretch of approximately 2.7 km is situated downstream of the dam and hydro-plant. The new lock approach is situated downstream of the existing ship lift approach and existing lock approach. The existing lock-emptying outlet is located upstream of the entrance of the common approach channel, whereas the new lock-emptying outlet is split into two sections: the outer river and the new lock approach (Figure 1).

To facilitate the investigation of water-level fluctuations in a branched lower approach channel system, several typical sampling sites are arranged in the multi-approach channels. For instance, the sampling sites 1#–5# are located in the ship lift approach channel, 6#–10# in the main approach channel (i.e., a common approach and an existing lock approach), and 11#–14# in the new lock approach channel. The arrangement of these sampling sites in a branched lower approach channel system is shown in Figure 1.

2.2. Establishment of hydrodynamic model

2.2.1. Governing equations

In modelling the waterway flow, with the assumption of hydrostatic pressure distribution and uniform distribution of hydraulic parameters along the vertical direction, a two-dimensional (2-D) shallow water equation is derived for the shallow waterway by depth-averaging the Reynolds-averaged mass and momentum conservation. The 2-D shallow water equation

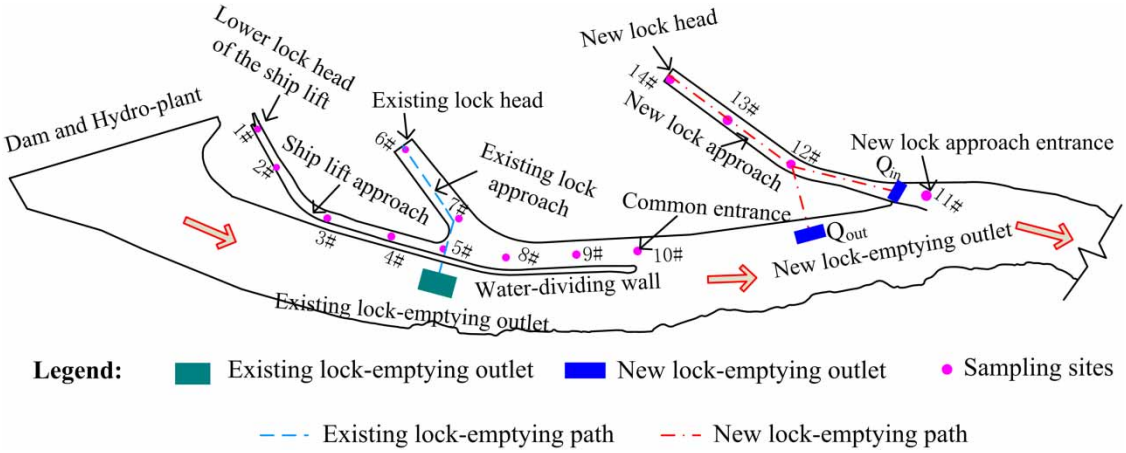

Figure 1 | Layout of the typical sampling sites in a branched approach channel system.

is as follows (without taking into account the effect of the Coriolis force and wind stress):

$$\frac{\partial \mathbf{q}}{\partial t}+\frac{\partial \mathbf{E}}{\partial x}+\frac{\partial \mathbf{G}}{\partial y}=\frac{\partial \overline{\mathbf{E}}}{\partial x}+\frac{\partial \overline{\mathbf{G}}}{\partial y}+\mathbf{S} \tag{1}$$

$$\mathbf{q}=\begin{bmatrix} h \\ hu \\ hv \end{bmatrix} \mathbf{E}=\begin{bmatrix} hu \\ hu^2+gh^2/2 \\ huv \end{bmatrix} \mathbf{G}=\begin{bmatrix} hv \\ huv \\ hv^2+gh^2/2 \end{bmatrix} \tag{2}$$

$$\overline{\mathbf{E}}=\begin{bmatrix} 0 \\ 2h\lambda_t \partial u/\partial x \\ h\lambda_t(\partial v/\partial x+\partial u/\partial y) \end{bmatrix} \overline{\mathbf{G}}=\begin{bmatrix} 0 \\ h\lambda_t(\partial u/\partial y+\partial v/\partial x) \\ 2h\lambda_t \partial v/\partial y \end{bmatrix} \mathbf{S}=\begin{bmatrix} S_q \\ gh(S_{ox}-S_{fx}) \\ gh(S_{oy}-S_{fy}) \end{bmatrix} \tag{3}$$

where $\mathbf{q}$ is the vector of conserved flow variables; $\mathbf{E}$ and $\mathbf{G}$ are the vectors of fluxes in the x and y directions, respectively; $\bar{\mathbf{E}}$ and $\bar{\mathbf{G}}$ are the diffusion terms in the x and y directions, respectively; $\mathbf{S}$ is the vector of the source term. t is time; x and y are the Cartesian coordinates; h is the water depth; u and v represent the depth-averaged velocity components in the x and y directions, respectively; g represents gravitational acceleration; λ_t is the horizontal eddy viscosity coefficient; S_{ox} and S_{oy} represent the bottom slope term of the x and y directions, respectively, S_{fx} and S_{fy} represent the friction slope of the x and y directions, respectively, and S_q is the flow of a control volume.

The governing equations are solved numerically based on the assumptions of Boussinesq and hydrostatic pressure. An approximate Riemann solver is utilized for the computation of the convective fluxes at the element interfaces, which makes it possible to handle discontinuous solutions. The spatial discretization of the equations is carried out using a cell-centered finite volume method, and the second-order spatial accuracy is achieved via employing a linear gradient reconstruction technique. The time integration of the governing equations is performed using the second-order Runge-Kutta method. Additionally, a second-order total variation diminishing (TVD) slope limiter is used to avoid numerical oscillations during the calculations (Erpicum *et al.* 2014).

The simulation starts with the time step set to 3 s. In addition, for beaches in the study area that rise and fall with river levels, the treatment approach of flooding and drying fronts is based on the work of Zhao *et al.* (1994) and Sleigh *et al.* (1998).

2.2.2. Boundary conditions and computational mesh

To investigate water level fluctuations in a branched lower approach channel system, it is vital to clarify the types of boundary conditions used in the current 2-D model. There are four types of boundaries: (i) the outflow boundary of the dam and hydro-plant is set as the flow boundary; (ii) the downstream boundary of the model is set as the water level boundary; (iii) the outflow boundary for the ship lock during emptying operations is considered as the flow boundary which is equivalent to a point source contributing to the continuity equation, and water is discharged into the ambient waters when the magnitude of the source is positive; and (iv) other boundaries are set as closed boundaries. In particular, the normal fluxes of all variables are forced to zero along the closed boundaries.

In the context of these complex boundary conditions, to adapt to the complex irregular terrain boundaries, an unstructured triangular grid is used in the computational domain. The mesh size varies with the width of the approach channel. To be specific, the mesh in areas where there is a large gradient of topography is locally encrypted, and the mesh size generally decreases from the approach channel system to the main river channel. The mesh scale of the approach channel system is around 5–15 m, and the mesh scale of the main waterway is around 20–50 m. Boundary conditions and mesh generation within the computational domain are depicted in Figure 2.

2.2.3. Model performance

To analyze model reliability, Root Mean Square Error (RMSE), Mean Absolute Percentage Error (MAPE), and Pearson Correlation Coefficient (R) are herein utilized to evaluate the model performance in this study, that is,

$$RMSE = \sqrt{\frac{1}{M}\sum_{i=1}^{M}(S_{mi} - S_{si})^2} \tag{4}$$

$$\mathrm{MAPE} = \frac{1}{M}\sum_{i=1}^{M}\frac{|S_{mi} - S_{si}|}{S_{mi}} \times 100\% \tag{5}$$

$$\mathrm{R} = \frac{\sum_{i=1}^{M}(S_{\mathrm{m}i} - \overline{S_{\mathrm{m}}})(S_{si} - \overline{S_{\mathrm{s}}})}{\sqrt{\sum_{i=1}^{M}(S_{\mathrm{m}i} - \overline{S_{\mathrm{m}}})^2 \sum_{i=1}^{M}(S_{\mathrm{s}i} - \overline{S_{\mathrm{s}}})^2}} \tag{6}$$

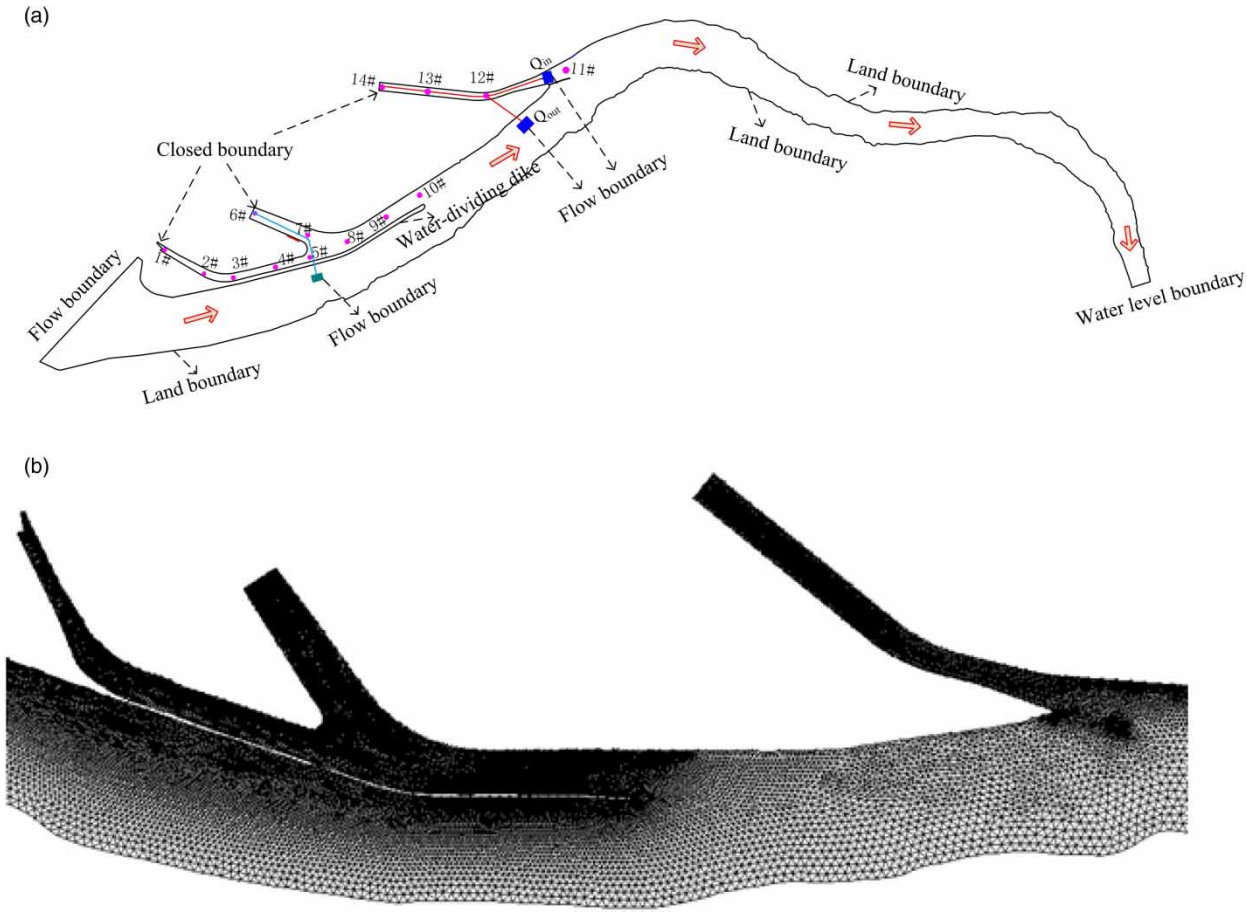

Figure 2 | Boundary conditions and mesh generation within the computational domain. (a) Boundary conditions; (b) Mesh generation of the branched lower approach channel system.

where M is the total number of samples; $\overline{S_m}$ and $\overline{S_s}$ are the mean of the measured and simulated data; S_{mi} and S_{si} are the measured and simulated values for the i-th time step, respectively.

2.3. Definition of the maximum amplitude of water level fluctuations

Given the fluctuation process at a typical sampling site in the lower approach channel, the maximum value (Δh_i, $i = 1, 2, 3\ldots, n$) among these amplitudes of water-level fluctuations was selected as the least favorable value for navigation safety by traversing the entire period T with the time window Δt. The maximum amplitude of water level fluctuations is defined by

$$\Delta h = \max\{\Delta h_1, \Delta h_2, \ldots, \Delta h_i, \ldots, \Delta h_n\} \tag{7}$$

The amplitude of water level fluctuations, in particular, is a critical parameter for the safe docking of the ship lift chamber during the safe operation period of the ship lift. The maximum hourly variation in water level at the lower lock head of the ship lift is less than or equal to 0.5 m, thus, the possibility of the ship lift chamber docking safely can be determined by comparing the actual maximum amplitude of water level fluctuations to the critical threshold.

3. RESULTS AND DISCUSSION

3.1. Model validation

Based on the case of the ship lock during emptying operations, when the initial time is at $t = 0$, the base flow is set to 5,000 m^3/s, and the initial water level elevation is set to 63.0 m. The occurrence time of peak value of the flow generated from lock operations is at $t = 306$ s. Noteworthy, base flow is regarded as constant during the entire operating phase of the ship lock. In this study, a dimensionless parameter (relative discharge ratio) is introduced to conduct the model validation, and the variation of the relative discharge ratio (ratio of the discharge (Q_t) to the maximum discharge (Q_0)) of the ship lock during emptying operations is shown in Figure 3.

To investigate water-level fluctuations in the lower approach channel induced by the new lock during emptying operations, a hydraulic physical model at a 1:80 scale and the numerical simulation were conducted in the context of a uniform condition (i.e., base flow discharged by the dam and hydro-plant was set to 5,000 m^3/s which remained steady during emptying operations of navigation lock, and the initial water surface elevation horizontal was at an elevation of 63.0 m). Figure 4 shows a comparison of the simulated and measured relative water depth (H_j/H_0, where H_0 is the initial water depth and H_j is the water depth at j-th moment) at the lower lock head of the ship lift, the existing lock head, the new lock head, and the entrance of the common approach channel.

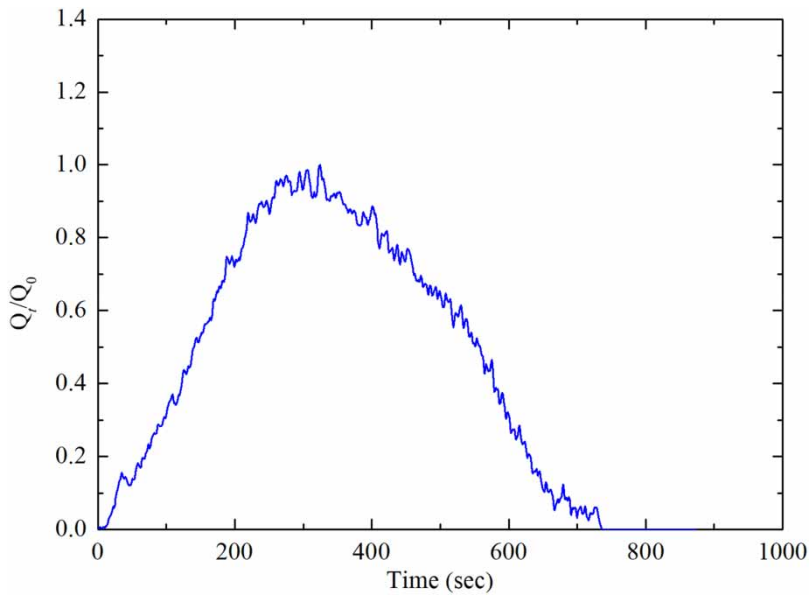

Figure 3 | Relative discharge ratio of the ship lock during emptying operations.

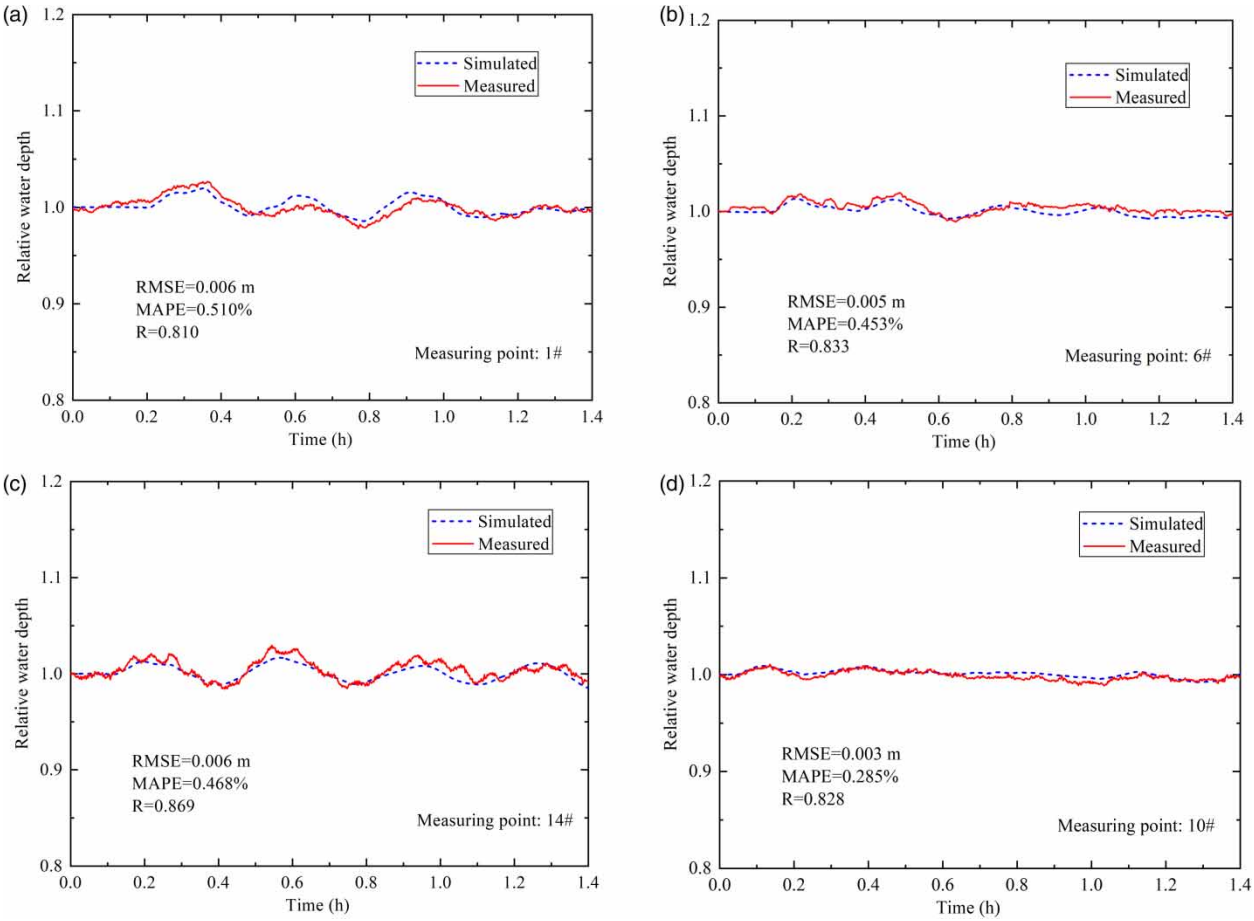

Figure 4 | Numerical simulation versus physical model test. (a) The lower lock head of the ship lift; (b) Existing lock head; (c) New lock head; (d) The entrance of the common approach channel.

As shown in Figure 4, the water level fluctuation process simulated using a two-dimensional hydrodynamic model is in good agreement with the overall trend of the physical model test data. For instance, the MAPE and the RMSE are less than 1.0% and 0.1 m, respectively, and the Pearson Correlation Coefficient is greater than 0.80. It demonstrated that the accuracy of the numerical model developed in this study could better simulate water-level fluctuations in a branched lower approach channel system. As a consequence, the numerical model could be used for subsequent research.

3.2. Spatial-temporal distribution of maximum water level variation

3.2.1. Uncertainty analysis on the flow generated by new lock operations

The release of water from a lock chamber is a transient process. In the field of navigational hydraulics, the flow process is commonly used to characterize the emptying operations of the lock. In the context of the unknown flow (Q_n (t)) generated by the new lock operations, the given flow process during existing lock operations can be derived from Figure 3. Then, we assume that Q_n is equal to 1, 1.2, 1.3, 1.4, and 1.6 times of the flow (Q_e) generated by the existing lock operations (i.e., $Q_n = 1$, 1.2, 1.3, 1.4, and $1.6Q_e$), respectively, sensitivity analysis on the discharge flow ratios of the new lock chamber to that of the existing lock chamber is conducted. The new dual-lane locks are operational with the base flow set to 5,000 m^3/s and the initial water surface elevation set to 63.0 m. The maximum water level variations within 5, 10, 15, 20, 25, 30, and 60 min are utilized to identify the relationship between maximum amplitude of water level fluctuations and relative discharge flow ratio ($Q_n/Q_e = 1$, 1.2, 1.3, 1.4, and 1.6) during the emptying operations of the new lock.

As shown in Figure 5, the discharge ratio of ship lock during emptying operations is linearly related to the amplitude of water level fluctuations within the same period, particularly for short times since the beginning of the emptying operations; the variation in water level at the lock head is rather sensitive to an increase in discharge, whereas the variation in water level at the entrance of the lower approach channel is minimal (around 0.15–0.17 m). For instance, if $Q_n = 1.0Q_e$, the maximum hourly variations in water level at the new lock head, the lower lock head of the ship lift, and existing lock head are 0.28, 0.22, and 0.14 m, respectively; if $Q_n = 1.6Q_e$, as the discharge outlet of the new lock during emptying operations is located near the entrance of the new lock approach, the maximum hourly variations in water level at the lower lock head of the new lock, the ship lift, and the existing lock reach 0.44, 0.34, and 0.22 m, respectively.

3.2.2. Spatial-temporal distribution of maximum wave amplitude

To identify the distribution pattern of the maximum variation in water level in a branched lower approach channel system, the discharge generated by the new lock during emptying operations is assumed to be 1.3 times higher than that generated by the existing lock operations. Figure 6 shows the water surface profile in the channel during the initial period of the lock during emptying operations (0–900 s), the maximum hourly fluctuation amplitude of the water level at typical sampling sites, and the water surface profile corresponding to the maximum and minimum water level at the lock heads (i.e., the lower lock head of the ship lift, the existing lock head, and the new lock head).

As shown in Figure 6(a), surges generated by the new lock during emptying operations reach the entrances of the common approach channel and new lock approach channel at 306 s, the wave propagates partly upstream and partly downstream,

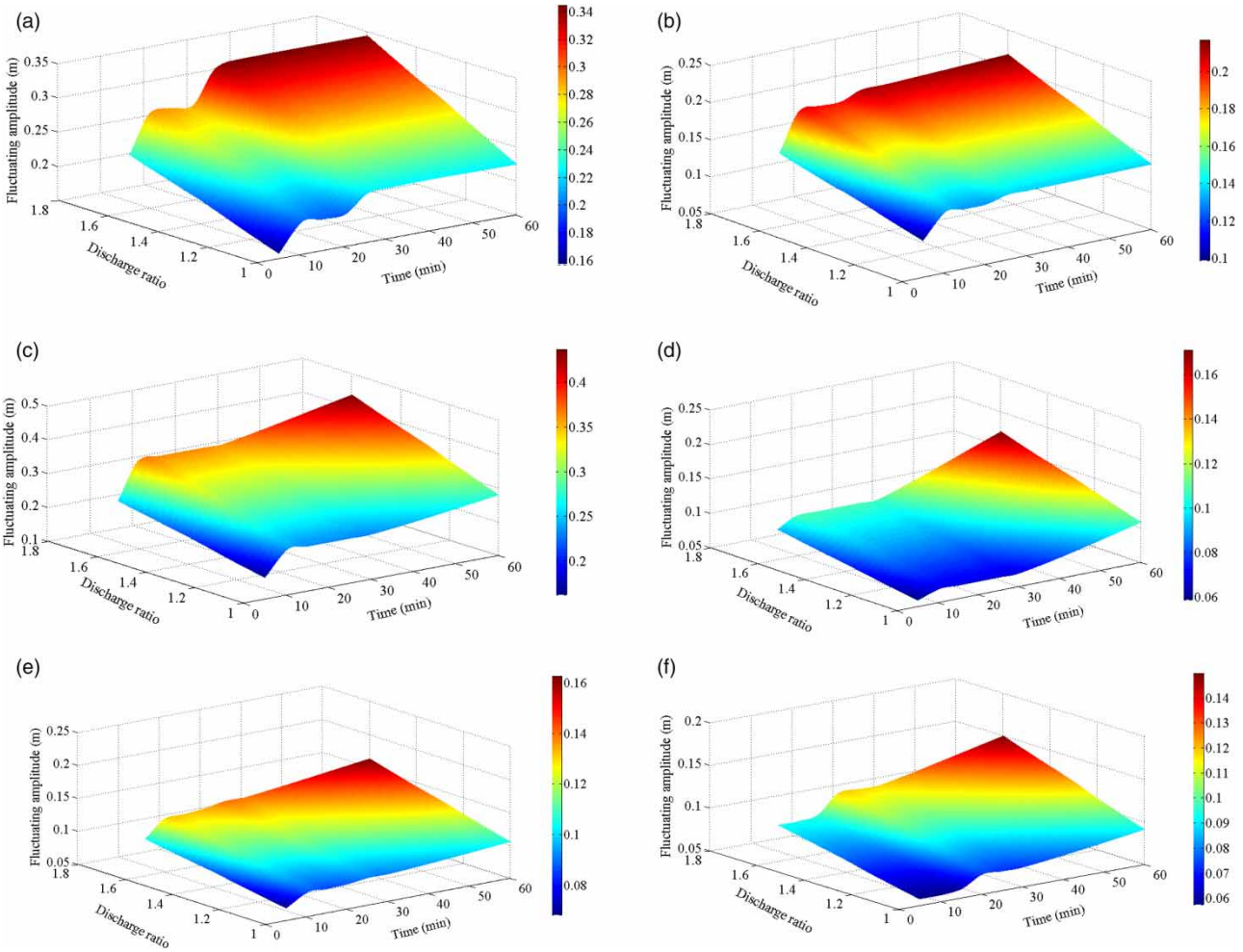

Figure 5 | Spatiotemporal distribution of maximum variation in water level in a branched lower approach channel system. (a) Lower lock head of the ship lift; (b) Existing ship lock head; (c) New ship lock head; (d) The entrance of the common approach channel; (e) The entrance of the ship lift approach; (f) The entrance of the new lock approach.

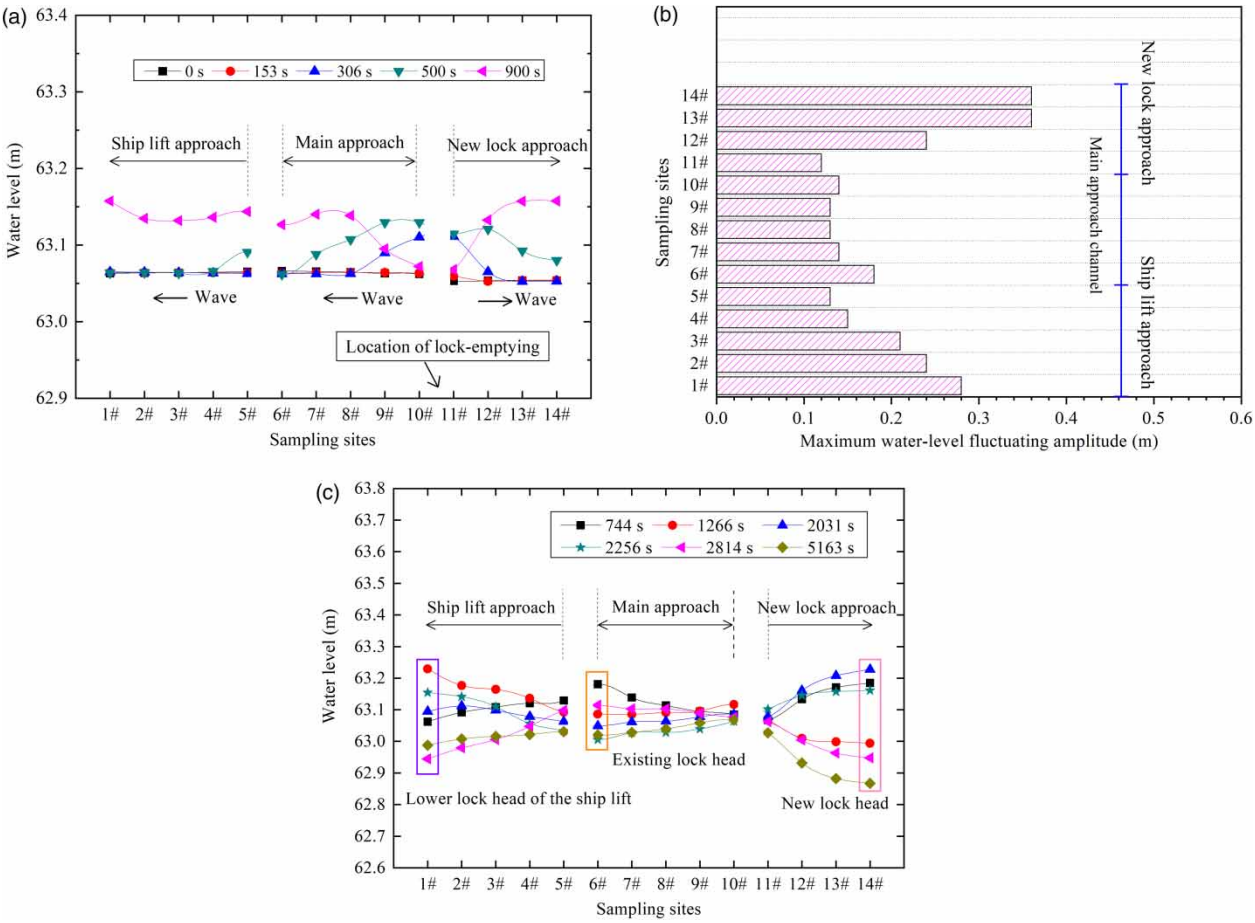

Figure 6 | Spatial distribution of water-level fluctuations and maximum water level variation in a branched lower approach channel system. (a) Water surface profile during the initial stage of lock operations; (b) Distribution of the maximum amplitude of water-level fluctuations; (c) Water surface profile corresponding to the maximum and minimum water level at the lock head.

reaching the entrances of the ship lift approach and existing lock approach at 500 s. As the wave profile evolves, the emptying operations of the lock ends around 800 s, and a wave profile develops in the lower approach channel around 900 s.

Figure 6(b) shows the distribution pattern of the maximum amplitude of water level fluctuations, the waves induced by lock operations have a significant impact on navigation safety, particularly the maximum amplitude of water level fluctuations at the ship lift approach (1# and 2#) and new lock approach (13# and 14#). Furthermore, the amplitude of water level fluctuations in the ship lift approach channel from the entrance to the lock head gradually increases; and the main approach (existing lock approach and common approach) and new lock approach have the greatest water level variations at the lock head. In addition, as shown in Figure 6(c), various wave profiles occur at different times. It denotes that the wave in the lower approach channel oscillates back and forth and is accompanied by energy transfer.

For simplicity, the subsequent research focuses on water-level fluctuations at the lower lock head of the ship lift (1#), the entrance of the ship lift approach (5#), the entrance of the common approach (10#), the existing ship lock head (6#), the new ship lock head (14#), and the entrance of the new lock approach (11#).

3.3. The amplitude of water level fluctuations in response to the interval running time of dual-lane locks

Existing dual-lane locks operation, existing single-lane lock and new single-lane lock operation simultaneously, and new dual-lane locks operation are examples of dual-lane lock operation patterns. Figure 7 presents the emptying operation modes of the dual-lane locks at various time intervals.

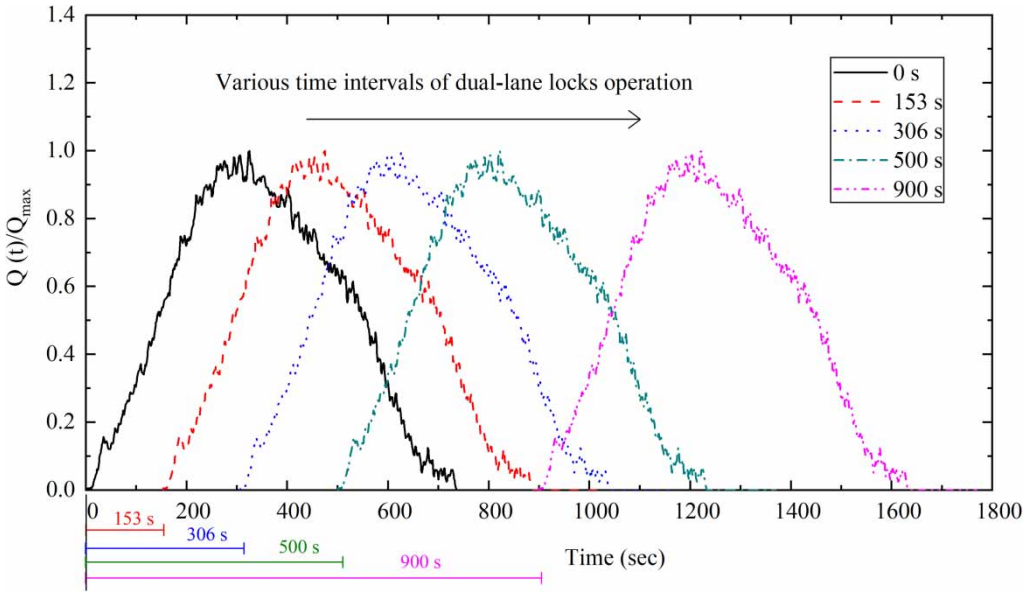

Figure 7 | Typical running modes of the dual-lane locks emptying at various interval times.

Assuming a base flow of 5,000 m^3/s and an initial water level of 63.0 m, the flow generated by the emptying operation of the new locks is approximately 1.3 times higher than that generated by the emptying operation of the existing locks. Three scenarios are considered herein based on the potential emptying operation modes of the dual-lane locks, the maximum hourly variations of the water level at the lock head and the entrance of the approach channel, as presented in Table 1.

3.3.1. Simultaneous emptying operation of dual-lane locks

The emptying outlet of the existing dual-lane locks operation is located upstream of the entrance of the common approach channel, with a positive wave bypassing the water-dividing wall and entering the common approach channel; while the wave negatively propagates into the common approach channel from the emptying outlet of new dual-lane locks, which is located downstream of the entrance of the common approach channel. Noteworthy, in the context of the simultaneous operation of the dual-lane locks, whether the emptying operation of the new and existing locks has an impact on water-level fluctuations in the approach channel needs to be studied in detail. In this study, to investigate the differences in water-level fluctuations in the

Table 1 | Maximum hourly water level variation at the lock heads and entrances (unit: m)

		Lock head			Approach channel entrance		
Scenario description	**Time interval (s)**	**Ship lift**	**Existing lock**	**New lock**	**Common**	**Ship lift**	**New lock**
Scenario 1: Existing dual-lane locks operation	0	0.25	0.17	0.15	0.12	0.13	0.10
	153	0.24	0.15	0.14	0.11	0.13	0.10
	306	0.18	0.14	0.10	0.12	0.08	0.08
	500	0.12	0.12	0.07	0.08	0.10	0.06
	900	0.17	0.13	0.10	0.07	0.11	0.07
Scenario 2: New single-lane and existing single-lane lock operation simultaneously	0	0.24	0.16	0.18	0.12	0.13	0.08
	153	0.24	0.16	0.18	0.12	0.13	0.09
	306	0.19	0.15	0.21	0.10	0.10	0.09
	500	0.19	0.15	0.25	0.08	0.10	0.06
	900	0.24	0.12	0.17	0.08	0.10	0.06
Scenario 3: New dual-lane locks operation	0	0.28	0.18	0.36	0.14	0.13	0.12
	153	0.26	0.15	0.34	0.13	0.12	0.11
	306	0.18	0.13	0.20	0.09	0.11	0.08
	500	0.23	0.16	0.25	0.12	0.12	0.09
	900	0.20	0.14	0.15	0.09	0.11	0.10

approach channel between the new dual-lane locks and existing dual-lane locks under operating conditions, we mainly focus on the amplitudes of water-level fluctuations at the typical sampling sites including the lock heads (the lower lock head of the ship lift, new ship lock head, and existing ship lock head) and the entrances (the entrance of existing lock approach, the entrance of new lock approach, and the entrance of ship lift approach). The maximum hourly variation in water levels at six sampling sites (Figure 1) under the different discharge ratios (i.e., $Q_n/Q_e = 1$, 1.2, 1.3, 1.4, and 1.6) can be obtained based on a 2-D hydrodynamic model, as shown in Figure 8.

As shown in Figure 8, water-level fluctuating amplitude in the approach channel shows a linear correlation with the discharge ratio of the new lock chamber to the existing lock chamber. In general, the amplitudes of water-level fluctuations at the entrances are small, and the amplitudes of water-level fluctuations at the lock heads are as follows: new lock head > lower lock head of the ship lift > existing lock head. In addition, as listed in Table 1, the amplitudes of water-level fluctuations corresponding to the scenario of new dual-lane locks operation are generally greater than that of the scenario of existing dual-lane locks operation. However, when the flow generated by the emptying operations of the new lock is equal to 1.15 times as much as the flow generated by the emptying operations of the existing lock, the amplitude of water-level fluctuation at the lower lock head of the ship lift reaches up to 0.25 m, which is equivalent to the amplitude of water level fluctuation in the context of existing dual-lane locks operation (Figure 8).

Additionally, as listed in Table 1, the amplitude of water level fluctuation at the new lock head is greater in Scenario 2 than in Scenario 1, and small differences in water level variation at other sampling sites can be found between the two scenarios as the emptying outlet location of the new lock is situated close to the new lock approach. Overall, the emptying operation of the dual-lane locks is relatively safe for navigation in a branched lower approach channel system.

3.3.2. Emptying operation of dual-lane locks at various time intervals

Except for Scenario 2, the water level variations at the lower lock head and the entrance of the lower approach channel have been reduced and water level variation at the lock head has altered significantly in the context of the emptying operation of dual-lane locks at various time intervals when compared to the simultaneous operation of the dual-lane locks. For instance, in Scenarios 1 and 3, the maximum decreasing amplitudes in the water level at the lower lock head of the ship lift are 0.13 and 0.10 m, respectively. Overall, the interval operating time of the locks is effective in reducing surges in a branched lower approach channel system, particularly at the lower lock head of the ship lift.

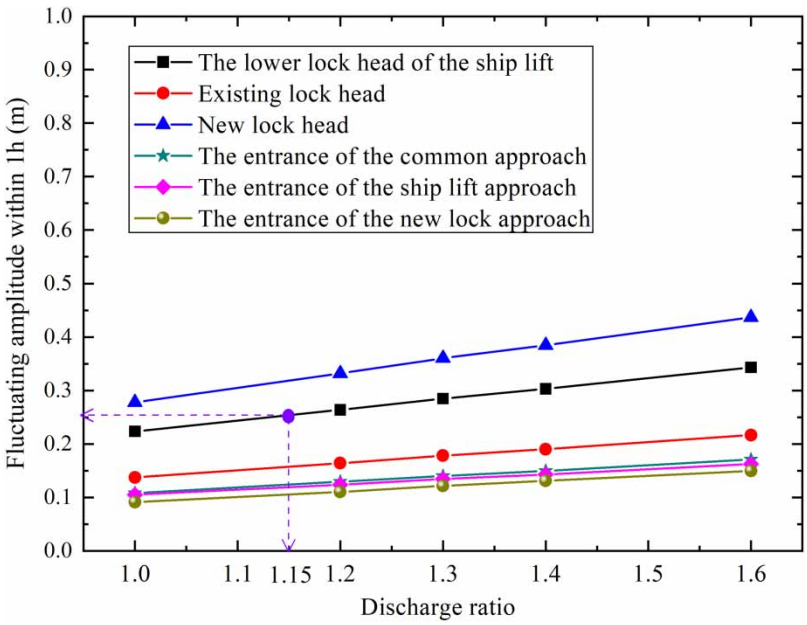

Figure 8 | Relationship between the maximum hourly variation in water level and the discharge ratio of the new lock chamber to the existing lock chamber under the emptying operation of new dual-lane locks.

3.4. Variation in water level in response to the emptying outlet locations of new lock

The outlet location of the new ship lock during emptying operations may change during the planning stage. For simplicity, the discharge generated by the new lock during emptying operations is assumed to be 1.3 times than that generated by the existing lock. This subsection considers the impact of various discharges generated by the new ship lock operations on water-level fluctuations in the approach channel. The outlet locations of the lock during emptying operations are shown in Figure 1. If the flow into the outer river is Q_{out} and the flow into the new lock approach channel is Q_{in} then the following relation is defined by

$$\alpha Q_{in} + \beta Q_{out} = Q_{tol} \tag{8}$$

where Q_{in} is the discharge into the new lock approach channel under the lock-emptying operations; Q_{out} is the discharge into the outer river, and Q_{tol} (Q_e) is the total discharge under the lock-emptying operations; α and β are the coefficients that meet $\alpha + \beta = 1$.

3.4.1. Emptying operations of the single-lane lock

In the context of single-lane lock operations, three scenarios are considered as follows: full discharge from lock chamber into the new lock approach ($\alpha = 1$ and $\beta = 0$), full discharge from lock chamber into the outer river ($\alpha = 0$ and $\beta = 1$), and 50% of the discharge from lock chamber into the outer river ($\alpha = \beta = 0.5$). The maximum hourly variation in water level at typical locations in a branched lower approach channel system is shown in Figure 9.

When the full discharge generated by the lock operations enters the outer river and the new lock approach, the deviations in the amplitude of water level fluctuations at the lower lock head of the ship lift are both minimal, whereas the latter ($\alpha = 1$ and $\beta = 0$) exhibits a larger variation in water level at the new lock head (around 0.39 m), which has a greater impact on the opening and closing of the mitre gates than that of the former ($\alpha = 0$ and $\beta = 1$). Furthermore, when 50% of the discharge generated by lock operations enters the new lock approach, the water level variation at the lower lock head of the ship lift is quite insignificant compared to other cases.

3.4.2. Emptying operation of the dual-lane locks

In the context of the simultaneous operation of the new dual-lane locks, assuming that the discharge ratios from the lock chamber into the outer river (Q_{out}) are set to 0%, 20%, 40%, 50%, 60%, 80%, and 100%, respectively, and the remaining discharge ratios into the new lock approach (Q_{in}) are set to 100%, 80%, 60%, 50%, 40%, 20%, and 0%, respectively. Table 2 presents maximum hourly amplitude in water level at various discharge ratios into the outer river at typical sampling sites.

The amplitudes of water level fluctuations at the entrances of the approach channel (ship lift approach, common approach, and new lock approach) are smaller regardless of how the discharge proportion into the new lock approach is distributed;

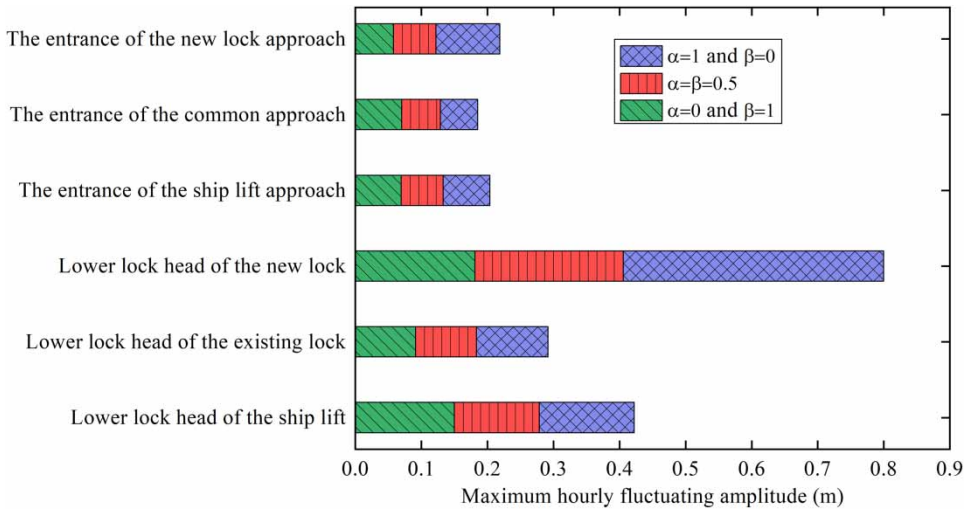

Figure 9 | Maximum hourly amplitude in water level at typical sampling sites in the lower approach channel system.

Table 2 | Maximum hourly water level variation for various discharge ratios into the outer river (unit: m)

Sampling sites	0%	20%	40%	50%	60%	80%	100%
Lower lock head of the ship lift	0.27	0.25	0.24	0.25	0.25	0.27	0.28
Existing lock head	0.21	0.20	0.19	0.18	0.17	0.16	0.18
New lock head	0.80	0.64	0.49	0.44	0.42	0.39	0.36
Ship lift approach channel entrance	0.14	0.13	0.13	0.13	0.13	0.13	0.13
Common approach channel entrance	0.11	0.11	0.12	0.12	0.12	0.13	0.14
New lock approach channel entrance	0.18	0.16	0.14	0.13	0.12	0.12	0.12

while the maximum variations in water level at the lock head are ranked as follows: new lock head > lower lock head of the ship lift > existing lock head. Notably, as the discharge ratio from the lock chamber into the outer river increases, the amplitude of the water level fluctuations at the new lock head gradually decreases; and the maximum hourly variation of the water level at the lower lock head of the ship lift exhibits a trend of first decreasing and then increasing, especially water level variation at the lower lock head of the ship lift reaches the minimum when the discharge ratio is approximately 40%. For instance, the maximum hourly water level variations at the lower lock head of the ship lift corresponding to the full discharge from the lock chamber into the outer river and the new lock approach are 0.28 and 0.27 m, respectively, and the maximum amplitudes of water level variations at the new lock head are 0.36 and 0.80 m, respectively. Generally, the amplitude of water level fluctuations at the lower lock head of the ship lift is not remarkable under the varied discharge ratios from the lock chamber into the outer river, whereas the amplitude of water level fluctuations at the new lock head is more significant.

3.5. Extreme scenarios of multi-lane locks operation

3.5.1. Simultaneous operation of the triple-lane locks

Assuming that the full discharge generated by the new dual-lane locks during emptying operations is released into the outer river (Figure 1), in the context of quadruple-lane lock group operations, there are two scenarios in which triple-lane locks are operating simultaneously, such as new dual-lane locks as well as existing single-lane lock operation simultaneously (marked as Scenario A), and existing dual-lane locks as well as new single-lane lock operation simultaneously (marked as Scenario B). Figure 10 shows the maximum water level variation at typical locations in a branched lower approach channel system within 5, 10, 15, 20, 25, 30, and 60 min.

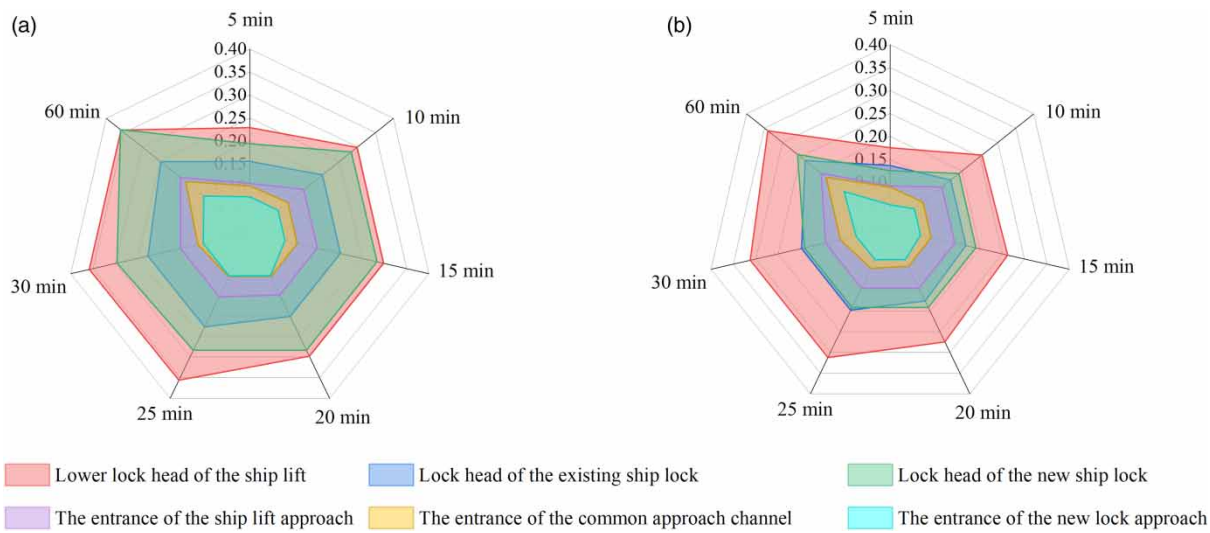

Figure 10 | Triple-lane locks operation. (a) New dual-lane locks as well as existing single-lane lock operation simultaneously (Scenario A); (b) Existing dual-lane locks as well as new single-lane lock operation simultaneously (Scenario B).

The maximum variation in water level in the lower approach channel occurs at the lower lock head of the ship lift followed by the new lock head; and the water level variations at the lock heads are generally greater than those at the entrances, as shown in Figure 10. Due to the proximity of the emptying outlet location of the new lock to the new lock approach, the maximum water level variation at the new lock head corresponding to Scenario A is greater than that of Scenario B. In particular, following the introduction of the new dual-lane locks, the maximum hourly variation of the water level at the lower lock head of the ship lift under the operation of triple-lane locks fulfils the standard for safe navigation of vessels.

3.5.2. Simultaneous operation of a quadruple-lane lock group

A typical quadruple-lane lock group consists of existing dual-lane locks and new dual-lane locks. A considerable water-level fluctuation may exhibit in the lower approach channel in extreme scenarios, making it impossible for ships to transit safely. Figure 11 shows the maximum variation in water level in the lower approach channel with the periods of 5, 10, 15, 20, 25, 30 and 60 min.

When quadruple-lane locks are in operation simultaneously, the maximum hourly variations in water level at the lower lock head of the ship lift, the new lock head, and the current lock head can reach 0.43, 0.37, and 0.32 m, respectively. Furthermore, the variations in water level at the lock heads are generally greater than at the entrances of the lock approaches. Overall, the simultaneous operation of a quadruple-lane lock group has little effect on the safe docking of the ship lift chamber.

3.5.3. The combination operation modes of quadruple-lane locks and hydropower units

The surges generated by the simultaneous operation of the quadruple-lane lock group may be superimposed on each other with the waves caused by the operation of the hydropower units. Therefore, assuming a base flow of 5,000 m^3/s and an initial water surface elevation of 63.0 m, the flow variation rates of load increment and load rejection for the unit are 1,000 $m^3/s/15$ min and 1,000 $m^3/s/5$ min, respectively. Several operation scenarios (i.e., Scenario D, Scenario E, and Scenario F) of the quadruple-lane lock group and the unit load peaking are shown in Table 3.

As shown in Table 3, the maximum hourly variation of the water level at the lower lock head of the ship lift meets the critical threshold value (0.5 m) in Scenario D; nevertheless, the wave induced by the hydropower unit peaking reaches the emptying outlet location of the existing locks and then quadruple-lane locks operation simultaneously, resulting in a maximum hourly variation of 0.49 m in water level at the lower lock head of the ship lift. Notably, for Scenario F, the maximum hourly variation in water level at the lower lock head of the ship lift has exceeded the critical threshold value (0.5 m) which should be avoided during the operations of quadruple-lane locks and hydropower units.

4. CONCLUSIONS

The amplitude of water-level fluctuations is vital to the docking and navigating for vessels in a branched lower approach channel system. In the context of the operation of quadruple-lane locks group, in this study, a typical branched lower approach

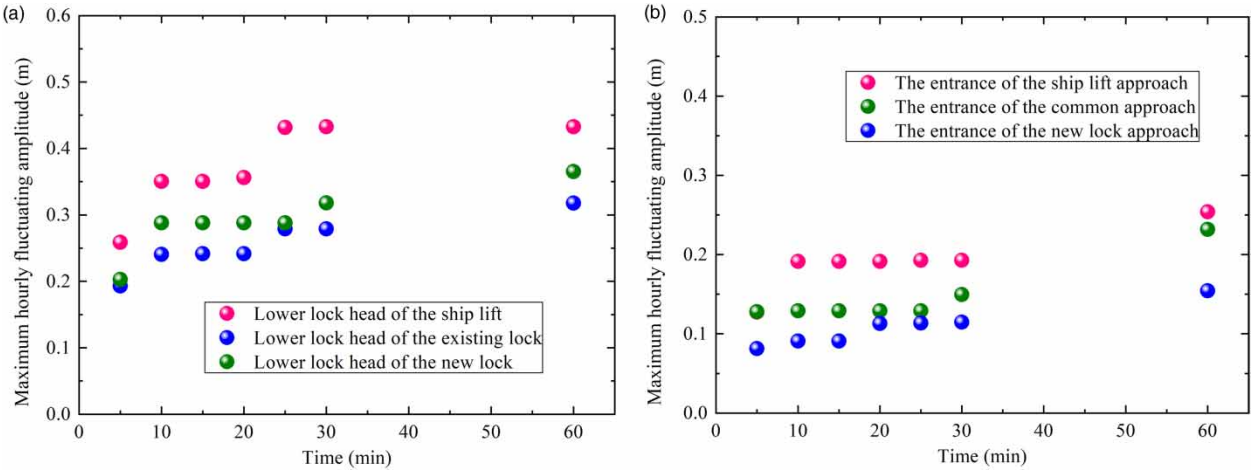

Figure 11 | Maximum amplitude of water level fluctuations. (a) Lower lock head; (b) The entrance of the approach channel.

Table 3 | Maximum hourly variation in water level under extreme operating scenarios (unit: m)

Scenario description	Flow variabilities of the unit	Lock head		
		Ship lift	Existing lock	New lock
Scenario D: unit load increment and quadruple-lane locks operation simultaneously	1,000 m^3/s/15 min	0.42	0.37	0.44
Scenario E: unit load increment, then lasts for 4 min, and quadruple-lane locks operation	1,000 m^3/s/15 min	0.49	0.40	0.40
Scenario F: unit load rejection and quadruple-lane locks operation simultaneously	1,000 m^3/s/5 min	0.52	0.46	0.49

channel system is selected as a study area, the water-level fluctuations in response to discharge, interval running time, and emptying outlet location of lock operations are investigated in details. In addition, extreme operation scenarios are identified to enhance the understanding of the water-level fluctuations at the lower lock head of the ship lift. The following conclusions can be drawn from this study:

1. With the increment of the discharge generated by lock operations, water level variation at the lock head is rather sensitive but at the entrance is insignificant; with the extension of the time operating interval of locks, the water level variation at the lower lock head of the ship lift can be reduced to a certain extent.
2. The maximum variations in water level at the lock heads are as follows: new lock head > lower lock head of the ship lift > existing lock head. With the increment of the discharge generated by the new lock operations, the water level variation at the lower lock head of the ship lift exhibits a trend of first decreasing and then increasing, and the water level variation at the lower lock head of the ship lift reaches the minimum when the outflow proportion of the outer river is around 40% of the total discharge generated by new dual-lane locks during emptying operations.
3. Triple- or Quadruple-lane locks operation simultaneously have less impact on the safe docking of the ships at the lower lock head of the ship lift. However, when quadruple-lane locks and the unit load rejection are in operation simultaneously, the water level variation at the lower lock head of the ship lift exceeds the critical threshold value, and thus the actual operation of the navigation lock group should be avoided in the future.

ACKNOWLEDGEMENTS

This work was funded by the National Key Research and Development Program of China (2016YFC0401906). The authors also want to thank the reviewers for their helpful suggestions and corrections on the earlier draft of our study according to which we improved the content.

CONFLICT OF INTEREST STATEMENT

The authors declare that they have no conflicts of interest.

DATA AVAILABILITY STATEMENT

All relevant data are included in the paper or its Supplementary Information.

REFERENCES

Baghlani, A. 2014 Water level stabilization in open channels using Chebyshev polynomials and teaching–learning-based optimization. *Journal of Hydroinformatics* **16** (5), 1097–1109.

Bravo, H. R. & Jain, S. C. 1991 Flow fields in lower lock approaches induced by hydro-plant releases. *Journal of Waterway, Port, Coastal, and Ocean Engineering* **117**, 369–389.

Deng, Y., Sheng, D. & Liu, B. 2021 Managing ship lock congestion in an inland waterway: a bottleneck model with a service time window. *Transport Policy* **112**, 142–161.

Erpicum, S., Pirotton, M., Archambeau, P. & Dewals, B. J. 2014 Two-dimensional depth-averaged finite volume model for unsteady turbulent flows. *Journal of Hydraulic Research* **52** (1), 148–150.

Li, F. & Sun, J. 1999 Research on navigation condition in lock downstream approach channel of TGP. *Journal of Yangtze River Scientific Research Institute* **16** (5), 13–16 (in Chinese).

Liang, D., Zeckoski, R. W. & Wang, X. 2014 Development of a hydro-environmental model for inland navigational canals. *Journal of Hydroinformatics* **16** (3), 572–587.

Liao, P. 2018 Improved analytical model for estimating the capacity of a waterway lock. *Journal of Waterway, Port, Coastal, and Ocean Engineering* **144** (6), 04018021.

Liu, Z., Ma, A. & Cao, M. 2012 Shuifu-Yibin channel regulation affected by unsteady flow released from Xiangjiba Hydropower Station. *Procedia Engineering* **28**, 18–26.

Maeck, A. & Lorke, A. 2014 Ship-lock-induced surges in an impounded river and their impact on subdaily flow velocity variation. *River Research and Applications* **30** (4), 494–507.

McCartney, B. L. 1986 Inland waterway navigation project design. *Journal of Waterway, Port, Coastal, and Ocean Engineering* **112** (6), 645–657.

MOTC (Ministry of Transport of China) 2001 *Code for Master Design of Ship Locks. JTJ 305-2001*. Standardization Administration of China, Beijing (in Chinese).

MTPRC (Ministry of Transport of the People's Republic of China) 2014 *Navigation Standard of Inland Waterway*, Beijing. (in Chinese)

Natale, L. & Savi, F. 2000 Minimization of filling and emptying time for navigation locks. *Journal of Waterway, Port, Coastal, and Ocean Engineering* **126**, 274–280.

PIANC (MarCom Working Group 30) 1995 *Joint PIANC-IAPH Report on Approach Channels–Preliminary Guidelines: Supplement to Bulletin No. 87*. PIANC General Secretariat, Brussels, Belgium.

Schindfessel, L., De Mulder, T., Creelle, S. & Schohl, G. A. 2014 On analytical formulae for navigation lock filling–emptying and overtravel. *Journal of Hydraulic Research* **53** (1), 134–148.

Shang, Y., Li, X., Gao, X., Guo, Y., Ye, Y. & Shang, L. 2017 Influence of daily regulation of a reservoir on downstream navigation. *Journal of Hydrologic Engineering* **22** (8), 05017010.

Sleigh, P. A., Gaskell, P. H., Berzins, M. & Wright, N. G. 1998 An unstructured finite-volume algorithm for predicting flow in rivers and estuaries. *Computers & Fluids* **27** (4), 479–508.

Stockstill, R. L., Park, H. E., Hite, J. E. & Shelton, T. W. 2004 *Design Considerations for Upper Approaches to Navigation Locks*. U.S. Army Engineer Research and Development Center, Vicksburg, MS.

Wilschut, T., Etman, L. F. P., Rooda, J. E. & Vogel, J. A. 2019 Similarity, modularity, and commonality analysis of navigation locks in the Netherlands. *Journal of Infrastructure Systems* **25** (1), 04018043.

Xu, J., Chen, Q., Li, Y., Zhou, J., An, J., Yan, X. & Guo, Y. 2018 Study on the hydrodynamic resistance moment of horizontally-framed miter gates. *Water* **10**, 1345.

Xue, A. Q. 1994 Experimental study on unsteady flow of downstream approach channel from locks of Three Gorges Project. *Journal of Yangtze River Scientific Research Institute* **11** (4), 10–15 (in Chinese).

Yang, Z., Zhu, Y., Ji, D., Yang, Z., Tan, J., Hu, H. & Lorke, A. 2020 Discharge and water level fluctuations in response to flow regulation in impounded rivers: an analytical study. *Journal of Hydrology* **590**, 125519.

Zhang, S., Jing, Z., Li, W., Wang, L., Liu, D. & Wang, T. 2019 Navigation risk assessment method based on flow conditions: a case study of the river reach between the Three Gorges Dam and the Gezhouba Dam. *Ocean Engineering* **175**, 71–79.

Zhao, D. H., Shen, H. W., Tabios III, G. Q., Lai, J. S. & Tan, W. Y. 1994 Finite-volume two-dimensional unsteady-flow model for river basins. *Journal of Hydraulic Engineering* **120** (7), 863–883.

Zhou, H.-x., Zheng, B.-y., Meng, X.-w. & Ge, L.-z. 2005 Influence of daily regulation of the three gorges power station on operating conditions of the approach channel. *Journal of Waterway and Harbour* **26** (1), 33–37 (in Chinese).

First received 7 December 2021; accepted in revised form 21 February 2022. Available online 7 March 2022